JOURNAL OF MATERIALS SCIENCE 19 (1984) 270–278

Microstructure of carbonaceous mesophase spherule

SHINJI HIGUCHI, RYOHEI OTSUKA
School of Science and Engineering, Waseda University, Okubo, Shinjukuku, Tokyo, Japan 160

MINORU SHIRAISHI
National Research Institute for Pollution and Resources, Yatabe, Ibaraki Japan 305

Carbonaceous spherules of mesophase were examined by transmission electron microscopy (TEM) and X-ray diffraction to precisely clarify its structure. A series of thin sections were cut from a single spherule with a microtome, and the three-dimensional lamellar structure of the spherule investigated. From 0 0 2 dark-field images and selected area electron diffractions (SAD), it was observed that the spherule was of the Brooks–Taylor type, with the lamellae being parallel even at the poles of the spherule. Structural changes within the spherule was studied following carbonization and graphitization. The structure of the resultant coke was essentially that of spherule of mesophase. Size of the lamellae increased as well as. The number of stacking lamellae also increased, but a rapid increase was not seen. The spherules of mesophase show a high degree of homogeneity and an excellent degree of graphitization.

1. Introduction

The carbonaceous mesophase spherule was first studied by Brooks and Taylor [1]. They suggested the model for the spherule microstructure in which the polyaramatic molecules were approximately parallel to one another and perpendicular to the surface of a spherule. Recently, Auguie *et al.* [2] proved the above model from their observation of thin sections of spherules with a transmission electron microscope. They also indicated that the carbonaceous mesophase belonged to a discotic liquid crystal.

The present work aimed to clarify more precisely the structure of the mesophase spherule by using a transmission electron microscope (TEM) and an X-ray diffractometer. So a series of continuous thin sections were cut from the same spherule with a microtome, then the three-dimensional lamellar structure of spherule was investigated. The structural transformation of spherules was also studied when carbonized and graphitized, and the spherule carbon were compared with the carbon obtained from the same starting material without the separation of the mesophase spherule.

2. Experimental details

2.1. Samples

A prydine soluble fraction of Kureha pitch (thermal cracked residues of crude oil) was heat treated at a rate of 3° C min^{-1} up to 410° C, and then, maintained for 90 min in an inert atmosphere. Mesophase spherules are obtained as the quinolin insoluble (QI) component of the carbonization products. The spherules were embedded in epoxy resins and cut into thin sections having a thickness of about 40 to 100 nm using a microtome for the observation with TEM.

Coke and carbon were prepared by heating the spherules up to 1200 and 2800° C, respectively. Moreover, another carbon was obtained by direct heating-treating carbonized products before the quinoline treatment of the same starting material up to 2800° C in order to compare it with spherule carbon.

0022–2461/84 $03.00 + .12

2.2. TEM

A conventional TEM used here is Hitachi H-500H with an accelerating voltage of 100 kV. An electron microscope technique such as selected area electron diffraction (SAD), bright- and dark-field image and lattice image were applied to the specimens. In the dark-field technique, the aperture was set paraxial in the back focal plane and the incident beam was tilted to let the scattered beam through the aperture so that the effect of the spherical aberration could be decreased in imaging. However, in poor crystalline materials such as carbonaceous mesophase, the reciprocal lattice points are elongated and the area possible to diffract can deviate to the great extent from the Bragg angle. Therefore, the dark-field imaging technique in the present work was enough only for tilting the incident beam to obtain a paraxial reflection, because it was not necessary for the specimen to be tilted. To clarify how lamellae incline to the incident beam, the specimen tilting method was also used.

2.3. X-ray diffraction

X-ray diffraction patterns of the mesophase and the coke were analysed according to the Fourier transformation method [3, 4] for the 0 0 2 bands to obtain the distribution of stacking height of lamellae. Average lamellar size was calculated by Diamond's method for the 11 bands [3–8]. X-ray parameters of the carbons were gained according to the standard method prescribed by the Japan Society for the Promotion of Science [9]. L_a, L_c, N and d_{002} are defined as shown in Fig. 1. ϵ is defined by the following equation

$$1/L_c = 1/L_0 + l\epsilon/4d_{002}$$

where L_c is crystallite size in the direction of the c-axis obtained from the observed $00l$ diffraction profile. L_0 is true size of crystallite in the direction of c-axis. By plotting l against L_c, ϵ is obtained as its slope and means the fluctuation of interlayer distances in the direction of the c-axis.

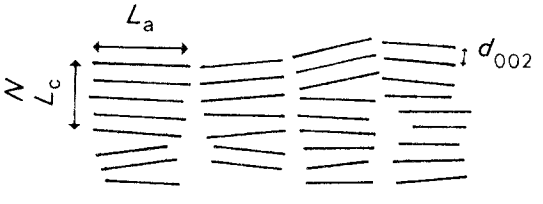

Figure 1 Definition of L_a, L_c, N and d_{002}. L_a and L_c are sizes of coherent domain in a- and c-axis direction, respectively, N average number of consisting of L_c, and d_{002} means interlayer spacing.

2.4. Optical diffraction

Optical diffraction is the diffraction of a laser beam by the negative of the micrograph. Just as in electron diffraction, the form of the optical diffraction pattern is directly related to the structural detail of the micrograph. So if the micrograph is of an amorphous specimen area and shows no periodic or regular detail, the optical diffraction pattern only contains a diffuse spectrum radially distributed about the central diffraction spot. If the specimen area is crystalline or the micrograph contain periodic detail, diffraction spots are observed in the optical diffraction pattern at the corresponding distances and orientations from the central diffraction spot.

3. Results

3.1. Mesophase

The mesophase used was nearly true spherular, less than 15 μm in diameter as shown in Fig. 2a. The optical anisotropy indicated that these were single spherules of non-coalesced mesophase. Each single spherule was cut at various positions parallel to each other and a series of thin sections, which contained the section cut at the polar plane, were obtained. Fig. 3 shows the 0 0 2 dark-field images of those sections, of which the sectioning positions in the spherule were determined from the sizes of the section and shown in Fig. 4. The bright regions indicate that 0 0 2 layer planes are satisfying the diffraction condition, and so layer planes were arranged almost perpendicular to the figure plane. In the section quite near the polar diameter (Fig. 3a), the bright dot region of the 0 0 2 dark-field images changed with the position of an objective aperture, shown in the inserted figure of Fig. 3a, on the 0 0 2 diffraction ring. From these dark-field images, the lamellar structure of the mesophase spherule can be described as in Fig. 4a. The 0 0 2 selected area electron diffraction (SAD) of the various positions in the same section indicates the lamellar arrangement agrees with the 0 0 2 dark-field images. The lamellae close to the surface of a spherule are arranged perpendicular to the surface around the equatorial plane, but they change their directions to an angle of 60°–70° to the surface when approaching the pole. Figs. 4b, c and d describe the lamellar arrangement when the structure is cut at each position in the spherule.

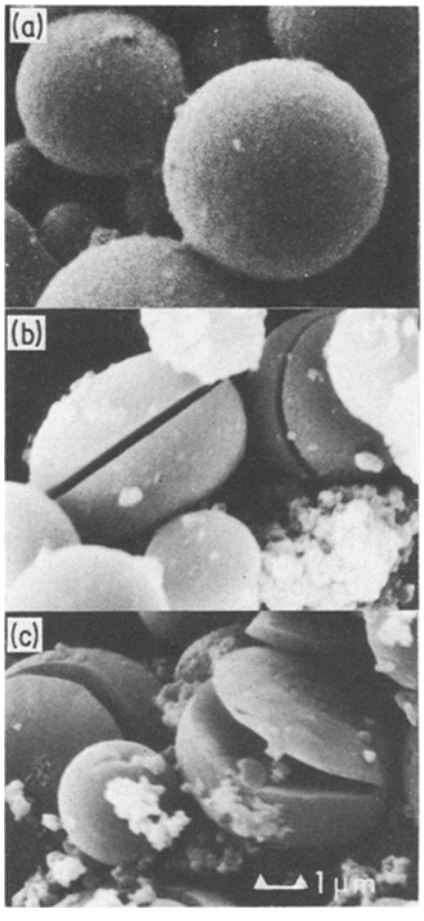

Figure 2 Scanning electron micrographs: (a) mesophase, (b) coke, (c) carbon.

A series of thin sections (Figs. 3b, c and d) cut parallel to the plane containing both poles show the changes in the bright region with the position of an objective aperture on the 0 0 2 diffraction ring. These changes in dark-field images and the lamellar arrangement which are obtained by the SAD patterns agree with Figs. 4b, c and d.

Fig. 5b shows the 0 0 2 dark-field image at higher magnification. The bright dots, of which the size corresponds to about 1 nm, are distributed homogeneously over an extensive area. The SAD pattern (Fig. 5a) shows a strong 0 0 2 arc which indicates considerable preferred orientation. The lattice image (Fig. 5c) shows roughly parallel fringes of about 1–2 nm over a very long range, although two successive stacks of fringes are very misoriented. Fig. 6 is the laser beam optical diffraction, using the negatives of the micrographs of the lattice fringes as the object. This (Fig. 6a) shows that the relative misorientation of the neighbouring scattering domains was about ± 20° and that the distribution of the interlayer spacing extends up to 0.6 nm, with the most frequent spacing being 0.35 nm, as can be seen in Fig. 7.

Fig. 8 shows X-ray profiles of the 0 0 2 bands, after the correction of polarization, absorption and atomic scattering factor of carbon, in the range of $s(s = 2 \sin\theta/\lambda$, where θ is half the diffraction angle and λ the wavelength used) values smaller than 0.45. The interlayer spacing d_{002} is 0.349 nm. A histogram of the stacking height is given in Fig. 9. Apart from the single occurring layers, the most frequently occurring groups contain two or three layers, with the average number of layers per stack being 2.7. An X-ray profile of the 11 bands corrected by the polarization factor and absorption is shown in Fig. 10 in the range of $s = 0.66$ to 0.96, from which the average layer size was obtained to be 1.1 nm.

3.2. Coke

Coke keeps its spherical morphology, scarcely fusing to each other during carbonization (Fig. 2b). But most of the spherules are cracked and slightly deformed into a flat configuration. The observation with a polarizing microscope indicates that the cracks in the coke spherules generally happen in the parallel direction of the basal plane.

Most of the SAD patterns (Fig. 11a) show more intense 10 and 11 rings than those of the mesophase. The width of the 0 0 2 arc decreases and its intensity becomes stronger. The 0 0 2 dark-field image (Fig. 11b) shows an almost similar picture to the one observed in the mesophase spherule, but the dots are much brighter. The lattice image (Fig. 11c) shows the development of the layers to about 2 nm, but does not show a significant increase in stacking. In optical diffraction (Fig. 6b), diffraction units are more intense and the distribution of the interlayer spacing (Fig. 7) is wider than in the mesophase.

The interlayer spacing d_{002} is 0.352 nm. The histogram of the layer stacking (Fig. 9) shows an increase in the groups containing four to five layers, with the average number of layers per stack being 2.8. The average layer size, L_a, obtained from the 11 bands (Fig. 10) was 2.6 nm.

3.3. Graphitized spherule

Graphitized mesophase spherule also shows a cracked and slightly deformed spherule (Fig. 2c).

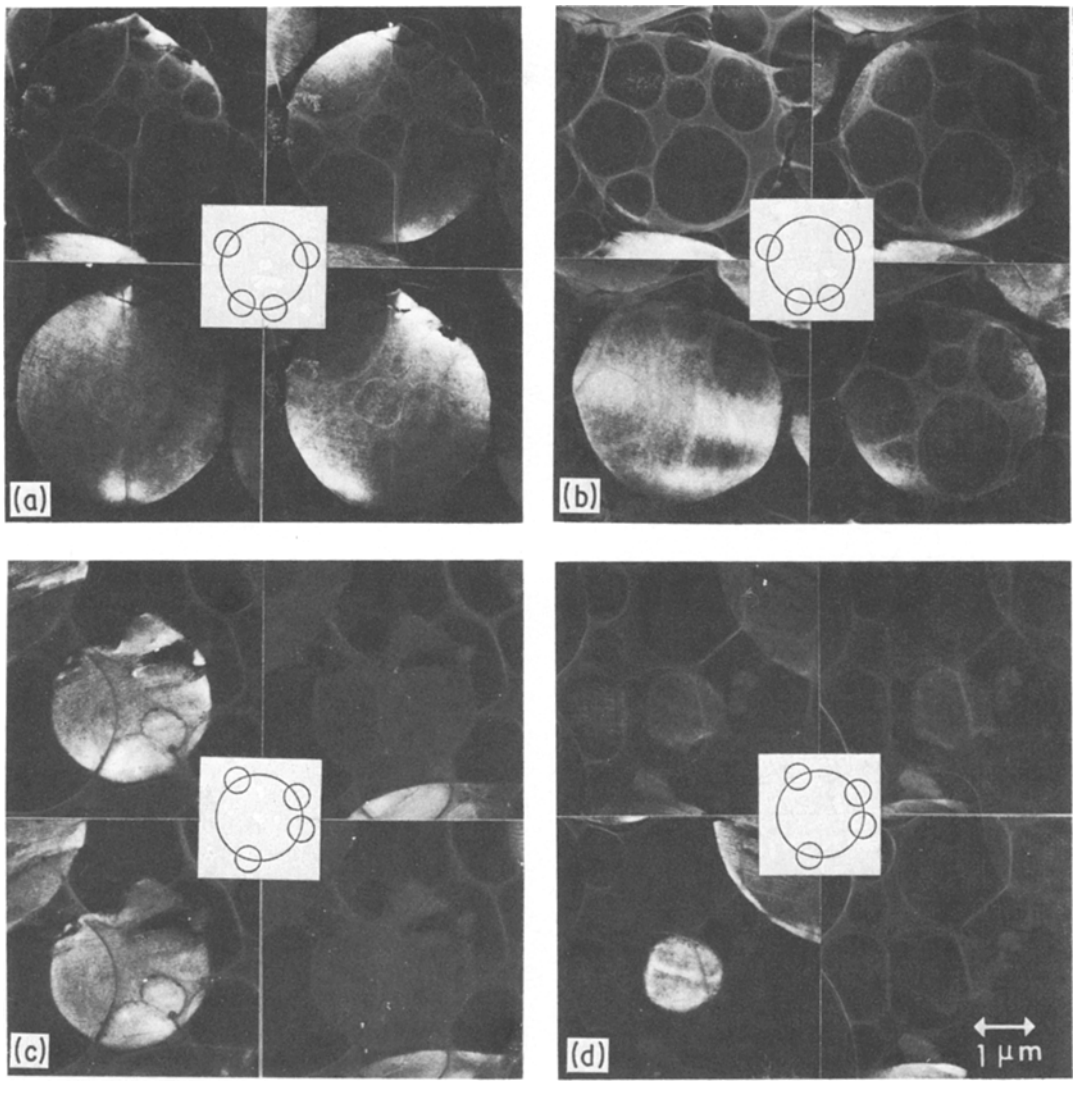

Figure 3 Mesophase: 0 0 2 dark-field images of a series of thin sections.

Ground samples are apt to lie for the most part on the sheet mesh as circular thin layers, of which the basal plane was found to be parallel to the sheet mesh by the SAD and dark-field image. Fig. 12a shows SAD pattern with dotted rings which indicate a rapid increase in crystallinity. It was evident from the 10 (Fig. 12b) or 11 dark-field images that the layer development was prominent. The 0 0 2 lattice image (Fig. 11c) showed large flat unconstrained layers, which are commonly produced in soft carbon.

X-ray diffraction parameters obtained from the 0 0 2 line and 1 1 0 line are as follows: $d_{002} = 0.3364$ nm, $L_{c002} = 75$ nm, $L_a > 100$ nm, lattice strain of c-axis direction $\epsilon = 0.010$.

X-ray parameters of the carbon obtained by direct heat treating without the quinolin treatment of the same starting material are as follows: $d_{002} = 0.3361$ nm, $L_{c002} = 80$ nm, $L_a > 100$ nm, $\epsilon = 0.0037$.

4. Discussion

4.1. Detailed analysis

4.1.1. Microstructure of mesophase spherule

The scattering domains in the mesophase were so small that the Bragg condition was no longer sharp. As the 0 0 2 resiprocal lattice point elongated, it can be demonstrated that the lamellae gave a 0 0 2 scattered beam even if lamellae were tilted ± 10°

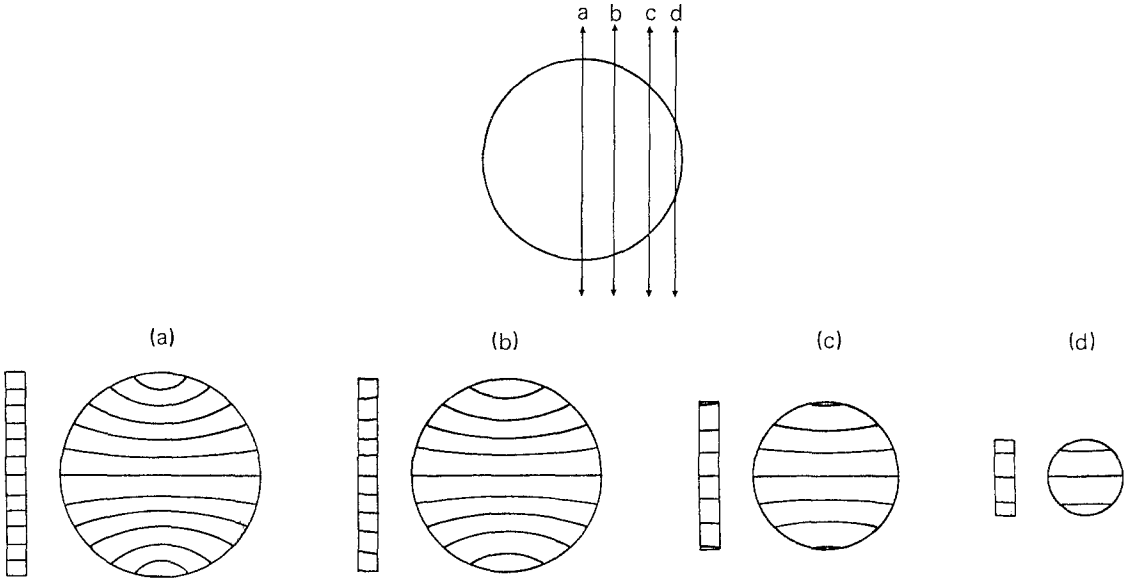

Figure 4 Structure of mesophase spherule inferred from the 0 0 2 dark-field image and SAD.

around the 0 0 2 Bragg angle, 0.3°, for the used wavelength [2]. Therefore, a region in which the lamellae have an angle of 100°–80° to the sectioned plane might still be bright in the 0 0 2 dark-field image. On the other hand, the misorientation obtained from the optical diffraction was about ± 20° as shown in Fig. 6. As there is no ordering of the lamellae on any of the planes containing an incident electron beam [10], the misorientation in the direction perpendicular to the sectioned plane was also about ± 20°.

In the 0 0 2 dark-field images of a series of thin sections (Figs. 3b, c and d), almost all of the regions in the sections brightened and satisfied Bragg's law. We observed that in the structure as shown in Fig. 4, the lamellae near the pole have an angle of 60°–70° to the sectioned plane. Considering the misorientation mentioned above, the angle of lamellae to the sectioned plane distributes to about ± 20° around an angle of 60°–70°, so it is possible that all the sectioned planes become bright in the 0 0 2 dark-field image. However, in the structure in which the lamellae were arranged perpendicular to the whole surface, the regions near both poles in the section could not satisfy Bragg's law, because the lamellae in those parts have an angle of 40°–50° to the sectioned plane [2] (shaded in Fig. 13). So considering the dark-

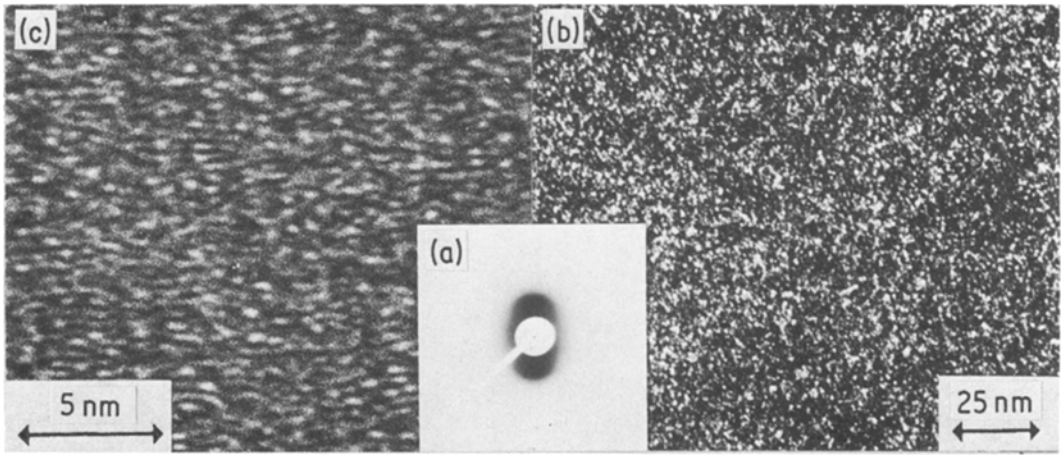

Figure 5 Mesophase: (a) SAD, (b) 0 0 2 dark-field image, (c) 0 0 2 lattice image.

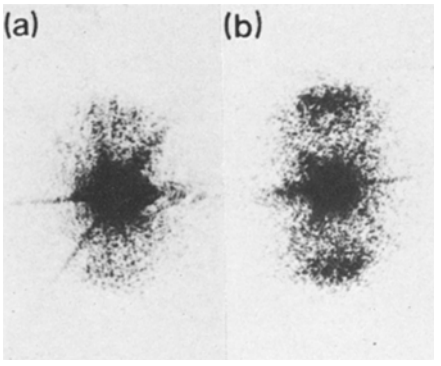

Figure 6 Optical diffraction: (a) mesophase, (b) coke.

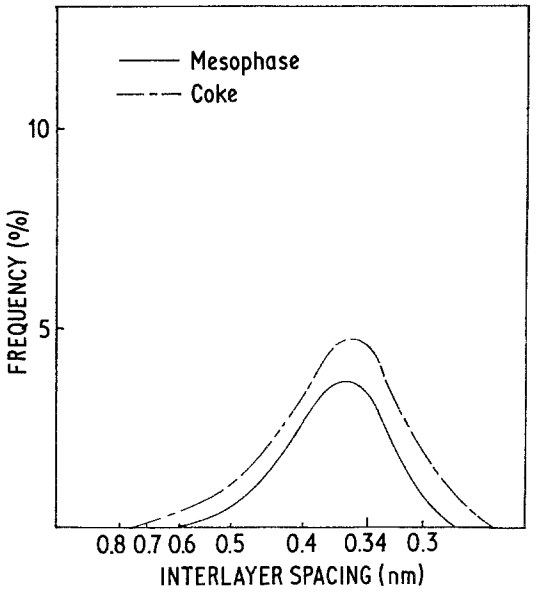

Figure 7 Distribution of interlayer spacing derived from optical diffraction.

field images (Fig. 3) and lamellar arrangement obtained by SAD of various positions in the same sections, a series of thin sections shown in Fig. 3 should have a microstructure as shown in Fig. 4.

4.1.2. Effect of the sectioning

To clarify whether the lamellae direction to the sectioned plane was altered after being cut by the microtome knife, the sectioned specimens were observed by the specimen tilting methods. When the section near the polar diameter was tilted to 20° in the direction of the movement of the knife, the bright dots in the 0 0 2 dark-field image disappeared. Even when tilted to 45° in the opposite direction, the image still lit up (Fig. 14). Considering that allowed angle of Bragg condition to the

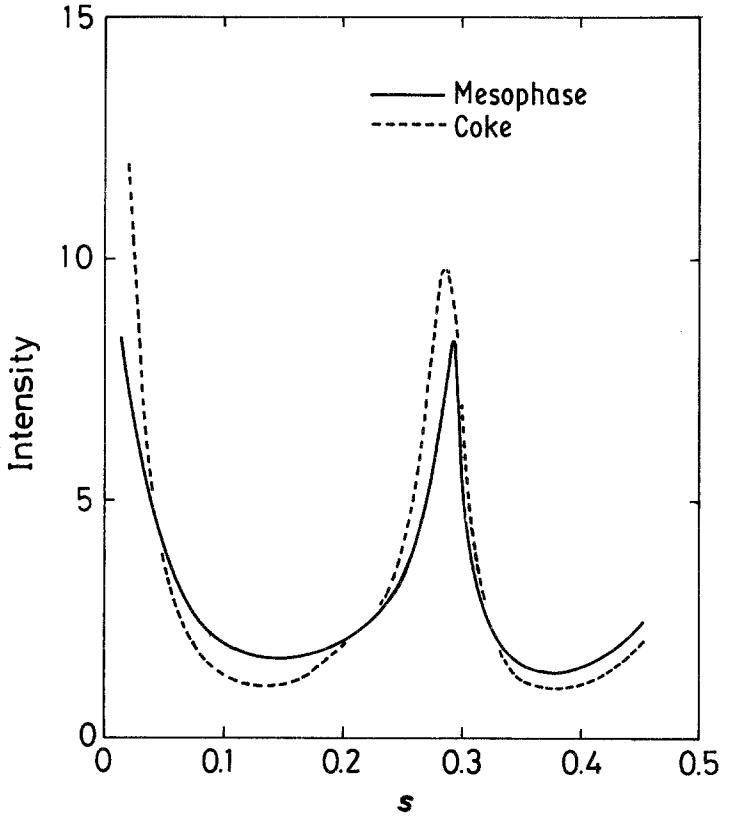

Figure 8 X-ray intensity curves for the 0 0 2 band of mesophase and coke.

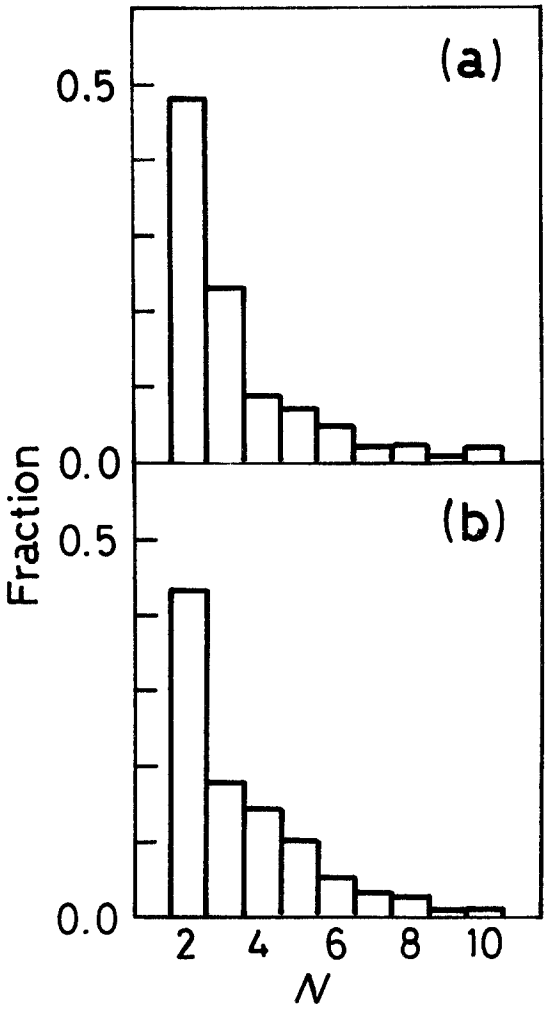

Figure 9 Histogram of stacking heights in mesophase and coke.

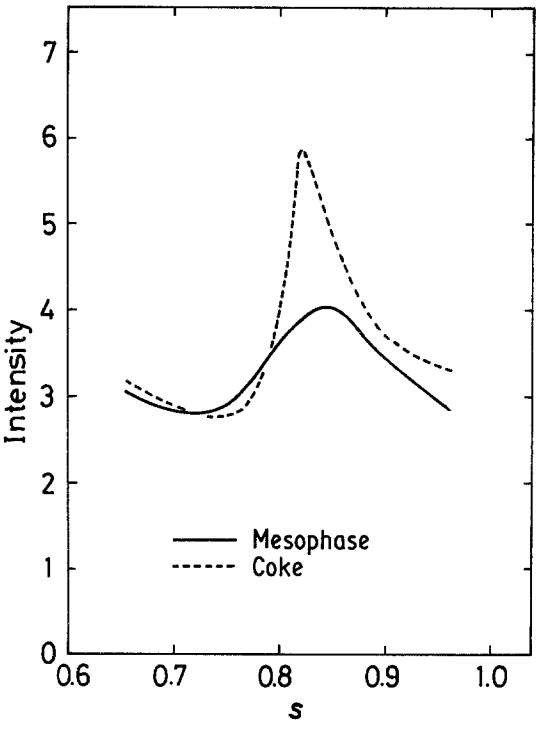

Figure 10 X-ray intensity curves for the 11 bands of mesophase and coke.

sectioned plane is 100–80° and the misorientation is about ± 20°, the angle of lamellae to the sectioned plane seemed to be altered in the direction of the movement of the knife to about 10°, as shown in Fig. 14. However, each relative position of the lamellae did not seem to be altered because the external form of the section did not change in shape.

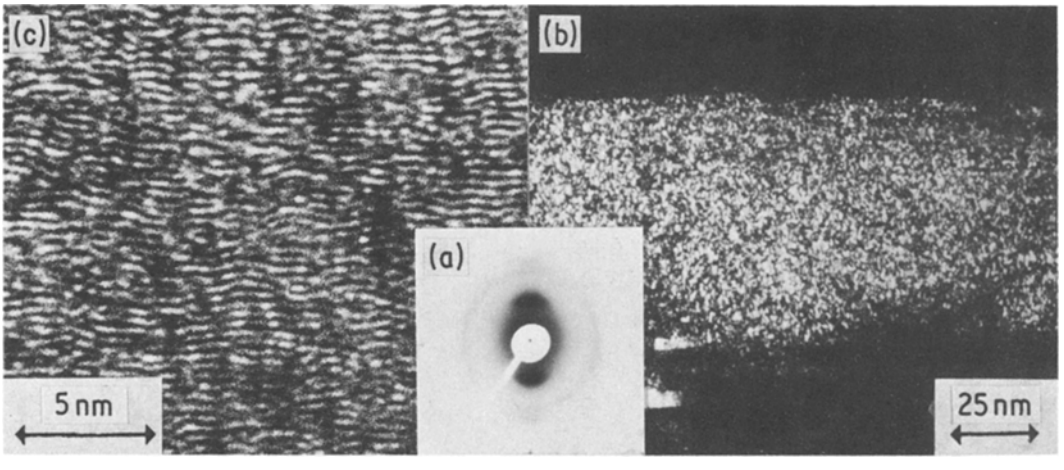

Figure 11 Coke: (a) SAD, (b) 0 0 2 dark-field image, (c) 0 0 2 lattice image.

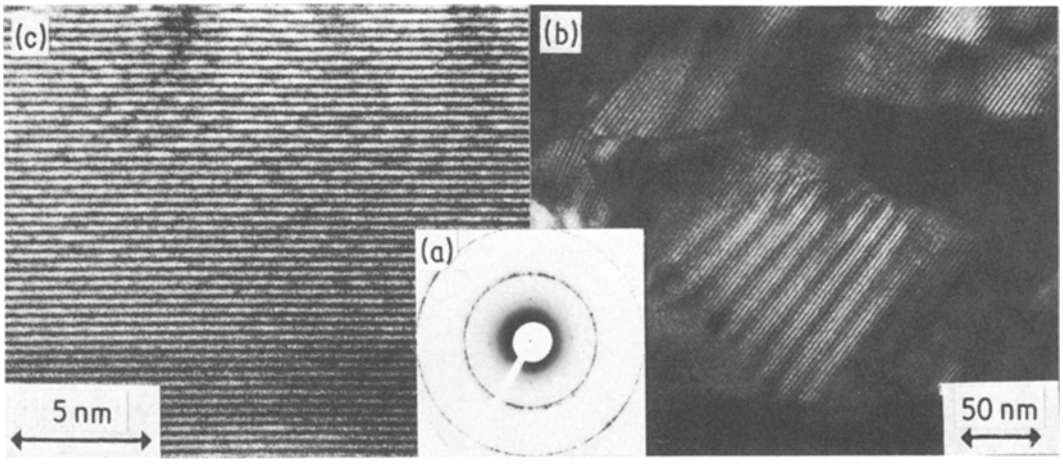

Figure 12 Carbon: (a) SAD, (b) 10 dark-field image, (c) 0 0 2 lattice image.

Although taking into account this alteration, the structure in which the lamellae were arranged perpendicular to the whole surface could not explain the 0 0 2 dark-field images shown Fig. 3. Because the angles of the lamellae to the sectioned plane changed from 40°–50° to 50°–60° near one of the poles, it might be possible to be brighten, considering the misorientation. But near the other pole of the same section, the angles were changed from 40°–50° to 30°–40°, so it was impossible to be brighter. On the other hand, the structure, obtained in this study, in which the lamallae has an angle of 60°–70° to the surface near the poles could explain the observed 0 0 2 dark-field images. Because the angles were changed from 60°–70° to 50°–60° near the one pole, from 60°–70° to 70°–80° near the other pole, therefore, all the sectioned planes could be brightened.

4.2. Structural change of mesophase spherule

4.2.1. Carbonization

The microstructure of coke was substantially equal to that of the mesophase, although there were recognized small changes in the structure. X-ray parameter L_a is 1.1 nm in mesophase and 2.6 nm in coke, 10 and 11 rings in the SAD patterns were more intense in coke than in mesophase and the lattice image also showed development of its layer size. For the development of L_a, each layer stack should have a change in its stacking axis, which brings about the development of layer stacking. But these structural transforms result in a wider distribution of the stack heights and cause a strain in stacking. Therefore, the 0 0 2 diffraction intensity and average number of layers per stack N were larger in coke than in mesophase, but the interlayer spacing and half intensity width of 0 0 2 diffraction patterns were larger in coke than in mesophase. The distribution of the layer spacings obtained from the optical diffraction was also wider in coke than in mesophase.

4.2.2. Graphitization

The graphitization of spherule carbon was investigated by a comparison with the carbon obtained without the quinoline treatment. X-ray parameters has similar values in both specimens except for the large value of the lattice strain in c-axis direction ϵ in the graphitized mesophase spherules. This means that the fluctuation of the layer spacing was larger in the graphitized mesphase than in the

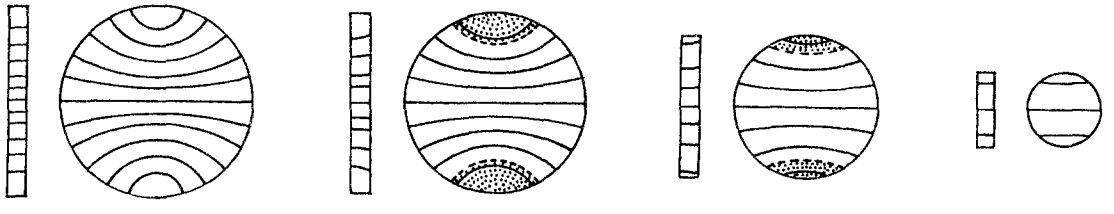

Figure 13 Structure of Brooks–Taylor's type. Sectioning position in the spherule are same in Fig. 4 [2].

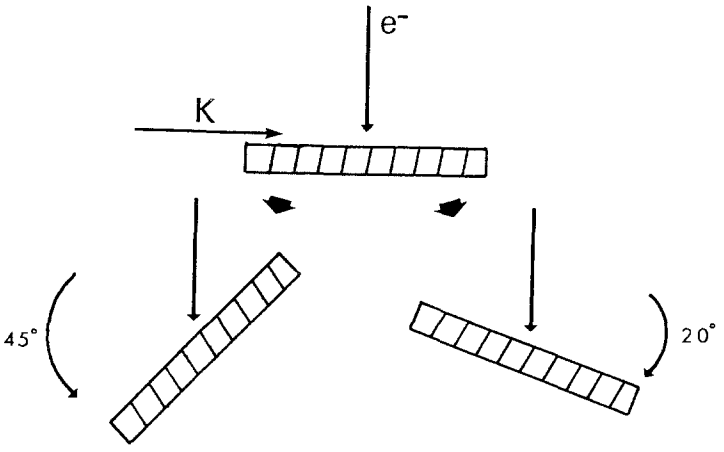

Figure 14 Specimen tilting method. e^- shows the direction of electron beam and K the direction of the movement of the knife.

other carbon. Carbon obtained from the mesophase spherule was carbonized and graphitized preserving its spherical shape without melting after the quinoline treatment, and consequently, layers should rest in bending near the poles even if cracks were formed in the spherules. Therefore, the fluctuation of the interlayer spacing was larger in the graphitized mesophase spherule than in the carbon obtained without the quinoline treatment [11]. Except for the above results, the X-ray parameters and observation of the graphitized mesophase with TEM were approximately the same as those of other graphitizing carbons, although carbonized and graphitized in the state in which small molecules did not coexist due to the quinoline treatment and did not melt.

5. Conclusion

The microstructure of the mesophase spherule corresponded basically to the Brooks–Taylor type, but the lamellae, of which the diameter was about 1 nm, were arranged more in parallel even near the pole; that is, the lamellae were arranged perpendicular to the surface around the equatorial plane and changed their directions to an angle of 60°–70° to the surface when approaching the pole.

The mesophase spherule indicate excellent degree of graphitization and homogeneity although it does not contain lower molecule, so does not melt during carbonization.

References

1. J. D. BROOKS and G. H. TAYLOR, "Chemistry and Physics of Carbon", Vol. 4, edited by P. L. Walker (Marcel Dekker, New York, 1968) p. 243.
2. D. AUGUIE, M. OBERLIN, A. OBERLIN and P. HYVERNAT, *Carbon* **18** (1980) 337.
3. R. DIAMOND, PhD dissertation, University of Cambridge, (1956).
4. *Idem, Phil. Trans, Roy. Soc. London* **A252** (1959) 193.
5. R. DIAMOND, *Acta Crystallogr.* **10** (1957) 359.
6. *Idem, ibid.* **11** (1958) 129.
7. M. SHIRAISHI and K. KOBAYASHI, *Nippon Kagaku Kaishi* (1972) 1135.
8. *Idem, Bull. Chem. Soc. Jpn.* **46** (1973) 2527.
9. 117 Conference of Japan Society for the Promotion of Science, *Tanso (Carbon)* **36** (1963) 25.
10. M. SHIRAISHI, G. TERRIERE and A. OBERLIN, *J. Mater. Sci.* **13** (1978) 702.
11. Y. YAMADA, K. KOBAYASHI, H. HONDA, M. TSUCHITANI and Y. MATSUSHIMA, *Tanso (Carbon)* **86** (1976) 101.

Received 7 February
and accepted 18 May 1983